# Temperature dependence and origin of InP(100) reflectance anisotropy down to 20 K

S. Visbeck* and T. Hannappel
*Hahn-Meitner-Institut Berlin GmbH, Glienicker Strasse 100, D-14109 Berlin, Germany*

M. Zorn† and J.-T. Zettler
*Institut für Festkörperphysik, Technische Universität Berlin, Sekr. PN 6-1, Hardenbergstr. 36, D-10623 Berlin, Germany*

F. Willig
*Hahn-Meitner-Institut Berlin GmbH, Glienicker Strasse 100, D-14109 Berlin, Germany*
(Received 20 December 2000; published 22 May 2001)

InP(100) surfaces were investigated by reflectance anisotropy spectroscopy (RAS) in the temperature range between 20 and 840 K. Surfaces were prepared via metal-organic chemical vapor deposition (MOCVD) resulting in P-terminated $(2\times1)$-like and In-terminated $(2\times4)$ reconstructions. Additionally, intermediate states of different phosphorus coverage were prepared. RA spectra were recorded both inside the MOCVD reactor and in an ultrahigh vacuum chamber. At low temperatures, features in the RA spectra sharpened significantly due to the reduced lattice vibrations and electron-phonon interactions. The temperature-dependent energy shift of specific RAS features was determined between 20 and 840 K, and fitted with a model containing the Bose-Einstein occupation factor for phonons. The respective fitting parameters were compared to those of the InP bulk critical-point transitions nearby. Careful data analysis provided evidence for surface transitions and surface modified bulk transitions in the RA spectra.

DOI: 10.1103/PhysRevB.63.245303 PACS number(s): 68.35.Bs, 81.05.Ea, 81.15.Gh, 78.66.Fd

## I. INTRODUCTION

Metal-organic chemical vapor deposition (MOCVD) is currently the preferred technique for growing III-V semiconductors. These materials find applications in a variety of devices, including light-emitting diodes, quantum-well lasers,[1] solar cells,[2,3] and high-speed transistors.[4,5] For these applications, InP(100)-based devices have become increasingly important. However, the electronic and atomic structure of InP(100) surfaces is not yet sufficiently investigated compared to GaAs(100) or Si(100). The knowledge of the properties of semiconductor surfaces and interfaces plays an important role for controlling the formation of hetero-interfaces of thin-film devices.[6,7] Recently, there has been major interest in the controlling of surface reconstructions and the stoichiometry of III-V interfaces by using reflectance anisotropy spectroscopy (RAS).[8–10] These investigations, however, were all carried out between room temperature and the growth temperature. This paper presents the first temperature-dependent RAS measurements of clean and well-ordered InP(100) surfaces from growth temperature down to 20 K using a recently developed system for contamination-free sample transfer from the MOCVD reactor to an ultrahigh vacuum (UHV) chamber.[8] The basic understanding of the physical origins of the characteristic RAS signatures is the focus of this paper. Our results complete the work presented in Ref. 9 where the reflectance anisotropy, the surface dielectric anisotropy, and the bulk dielectric function was established in the temperature range between 300 and 875 K.

Recently, Schmidt *et al.*[11] calculated the RA spectrum of the indium-rich $(2\times4)$ reconstructed InP(100) surface combining *first-principles* calculations with self-energy corrections. The calculated spectrum showed an amazing similarity with the experimental spectrum recorded at 20 K. The origin of the low-energy anisotropy around 1.9 eV was attributed to transitions occurring between surface states originating from the topmost atomic layers. Nevertheless, they could not reproduce all the spectral features in this region. For gallium arsenide, Berkovits *et al.*[12] could relate features in the RA spectrum to bulklike optical transitions. Even in the early 1980's, Aspnes and Studna[13] discriminated between ''intrinsic'' RAS contributions from surface effected bulk transitions and ''extrinsic'' contributions related only to the surface structure. In this paper, optical transitions from surface states into surface states (''ss transitions'') and surface-to-bulk (''sb''), bulk-to-surface (''bs''), and surface-modified bulk-to-bulk (''sm-bb'') transitions are identified by elucidating the temperature-dependent energy shift of the RAS signatures in the range from 20 K up to the growth temperatures ($\simeq$840 K). The temperature dependence of semiconductor bulk transitions is caused predominantly by the electron-(bulk)-phonon interaction.[14] For ss transitions, a different temperature dependence is expected, because in this case, the local surface phonon modes give the dominant contribution to the observed energetic shift and broadening.

In this paper, the line shapes of the different RA spectra recorded at 20 K and the surface dielectric anisotropy (SDA) calculated using the bulk dielectric function[15] are discussed and compared to experimental as well as calculated spectra from the literature. Afterwards, the temperature dependence of pronounced feature positions in the RA spectra from well-ordered In-rich $(2\times4)$ reconstructed surfaces and P-rich $(2\times1)$-like reconstructed surfaces are presented and compared to the bulk critical-point transitions nearby.

## II. EXPERIMENT

Clean and adsorbate-free InP(100) surfaces have been prepared under gas phase conditions in a horizontal Aixtron

 ©2001 The American Physical Society

AIX-200 reactor. The system was modified to achieve contamination-free sample transfer from the reactor to UHV (Ref. 16) and equipped with a LayTec RA spectrometer.[17] After oxide desorption, InP layers were grown using trimethylindium (TMIn) and tertiarybutylphosphine (TBP) as precursors. The following conditions were used during the growth: 850 K, 10 kPa of hydrogen, a growth rate of 1.8 $\mu/h$, a V:III ratio of 12.5, and a total flow rate of 5.5 l/min (at 25 °C and 1 atm). Sample handling and the procedure of the MOCVD to UHV transfer have already been described earlier.[8] P-rich surfaces were achieved by stabilizing the samples during the cool-down phase after growth until 625 K with a TBP partial pressure of 20 Pa. Less P-rich surface stoichiometries were achieved by annealing the samples after growth at different temperatures in the MOCVD reactor. RA spectra were recorded in the MOCVD environment between 840 K and room temperature. For low temperature measurements, the samples were mounted on top of the cold finger of a He cryostat inside the UHV system ($p<5\times10^{-9}$ Pa). The samples were cooled down to 20 K and warmed up stepwise to 400 K using the heater and temperature controller of the cryostat (Oxford ITC 502). At each step, RA spectra were taken after a waiting period of 15 min to allow the temperature to stabilize.

The RA spectrometer was attached to the MOCVD reactor and the UHV system via strain-free optical windows and with an orientation of the light polarizing axes at an angle of 45° to the two main crystalline axes $[0\bar{1}1]$ and [011]. The reflectance anisotropy of the InP(100) surfaces was measured as the difference between these two axes,

$$\frac{\Delta r}{r} = 2\frac{r_{[0\bar{1}1]} - r_{[011]}}{r_{[0\bar{1}1]} + r_{[011]}}, \tag{1}$$

using a setup according to Haberland *et al.*[17] Signatures in the measured RAS $\mathrm{Re}(\Delta r/r)$ spectra are only similar to those of the absorption anisotropy $\mathrm{Im}(\Delta\epsilon_s)$ of the surface region in spectral regions of low bulk absorption, where $\epsilon_b$ is real. Therefore, the surface dielectric anisotropy (SDA) $\Delta\epsilon_s d$ is usually calculated from the RA spectra using the bulk dielectric function:[18]

$$\Delta\epsilon_s d = \frac{\lambda(\epsilon_b - 1)}{4\pi i}\frac{\Delta r}{r}, \tag{2}$$

where $\epsilon_b \cong \langle\epsilon_b\rangle$ is the measured bulk dielectric function, $d$ is the effective thickness of the anisotropic surface layer ($d \ll \lambda$), and $\lambda$ is the wavelength of the light.

## III. RESULTS AND DISCUSSION

### A. RAS and SDA line shapes

Figure 1 shows RA spectra of InP(100) surfaces with varying phosphorus coverage at 20 K. These spectra can be correlated to the following surface reconstructions:[9,19] In-rich $(2\times4)$ (1), P-rich $(2\times1)$-like (3), and an example of an intermediate phase (2). The spectrum of the intermediate phase can be fairly well reproduced as a linear combination of the $(2\times4)$-related (52,5%) and the $(2\times1)$-like (47,4%) spectra (dashed line). Thus, the corresponding surface is more likely to consist of $(2\times4)$- and $(2\times1)$-like reconstructed domains[20] than a well-ordered reconstruction like the $\sigma(2\times4)$-phase recently found by Li *et al.*[21] RA spectra of the $(2\times4)$- and the $(2\times1)$-like reconstructed surface measured at different temperatures between 20 and 840 K are shown in Fig. 2.

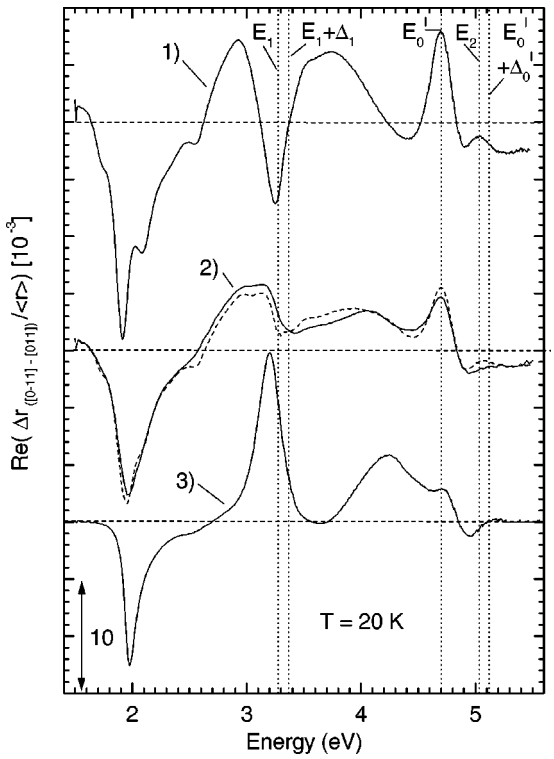


FIG. 1. RA spectra at 20 K of reconstructed InP(100) surfaces with different phosphorus coverage: In-rich $(2\times4)$ (1), P-rich $(2\times1)$-like (3), and a surface with an intermediate P-coverage (2). For comparison the energetic positions of the bulk critical point transitions $E_1$, $E_1+\Delta_1$, $E_0'$, $E_2$, and $E_0'+\Delta_0'$ are shown. Note that the intermediate spectrum can be reproduced as a linear combination of the $(2\times4)$-related (52,5%) and the $(2\times1)$-like (47,4%) spectra (dashed line).

At low temperature, the RA spectra show a significant blueshift and sharpening of the structures compared to the spectra taken at higher temperatures. These well-known effects are due to the reduced lattice constant and electron-phonon interactions.[22]

Figure 3(a) shows the bulk dielectric function taken from Ref. 15, Fig. 3(b) shows the SDA calculated with Eq. (2) from the RA spectra shown in Fig. 1. In contrast to the as-measured RA spectra, these SDA spectra mirror only surface optical properties. The wide peak above the $E_1+\Delta_1$ transition of all RAS spectra disappears in the corresponding SDA spectra. Furthermore, the strong peak at the $E_0'$ transition mainly visible in the $(2\times4)$ RA spectrum also changes to a smaller, derivativelike structure. The features at lower photon energies, however, are similar in the RAS and SDA spectra. Thus, our discussion of the temperature dependence of the RAS-related features will focus on the lower-energy part of the spectra.

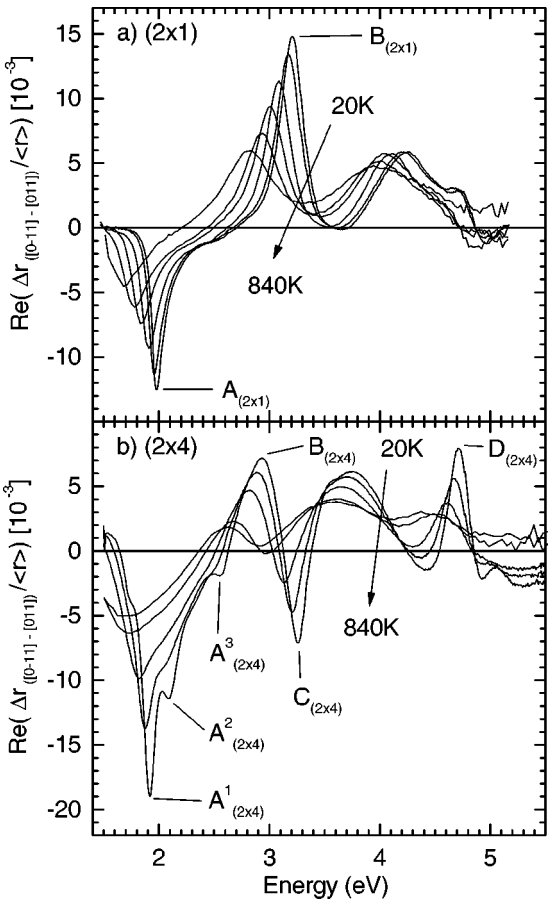


FIG. 2. RA spectra of the P-rich $(2\times1)$-reconstructed surface (a) and the In-rich $(2\times4)$-reconstructed surface (b) measured between 20 and 840 K. The temperature dependence of the energetic position of the respective features $A$–$D$ of the RA spectra is shown in Fig. 4.

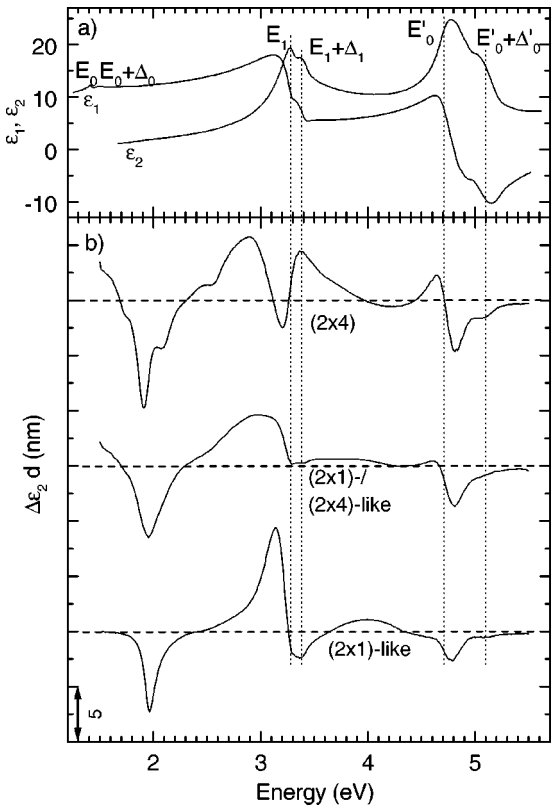


FIG. 3. (a) Real $(\epsilon_1)$ and imaginary $(\epsilon_2)$ part of the InP bulk dielectric function at 30 K. (Ref. 15) (b) Imaginary part of the surface dielectric anisotropy (SDA) of the different InP(100) surfaces at 20 K. The energetic positions of the bulk critical points $(E_1,\ E_1+\Delta_1,\ E_2,\ E_0',$ and $E_0'+\Delta_0')$ are indicated.

In addition to the sharpening of the spectral features, some new features appear in the spectrum of the well-ordered $(2\times4)$-reconstructed surface: a shoulder at 1.75 eV, two minima (labeled $A^2_{(2\times4)}$ and $A^3_{(2\times4)}$ in Fig. 2) at 2.09 and 2.55 eV, and a maximum around 5.03 eV.

As mentioned above, SDA spectra do not include the simple optical contribution of the bulk dielectric function to the surface optical response. Now, we focus on the physical origin of the signatures in the SDA spectra that can have either a pure surface transition (ss) character or can also involve extended bulk states by sb, bs or sm-bb transitions. We consider two different experimental observations to indicate that a specific SDA signature corresponds to a pure ss transitions: (a) there is no bulk critical point transition at the respective photon energy and (b) the $T$-dependence of neighboring bulk and SDA signatures is strikingly different. It should be noted that in general, point (a) does not exclude pure ss transitions in the vicinity of bulk critical points.

The energetic positions of the bulk critical-point transitions $E_1$, $E_1+\Delta_1$, $E_2$, $E_0'$, and $E_0'+\Delta_0'$ are shown in Fig. 1 and Fig. 3 as determined by Lautenschlager *et al.*[15] While there is no bulk transition in the energy region between 1.6 and 3 eV, most of the spectral features above 3 eV are obviously in close vicinity to one of the critical points as indicated in Fig. 1.

In the case of gallium arsenide, the coinciding room-temperature bulk critical point and RAS feature at 4.5 eV have been interpreted by Berkovits *et al.*[12] as a strong influence of the bulk dielectric properties on the reflectance anisotropy. Nevertheless, for InP other experimental findings support a clear surface contribution to the spectra, as can be seen around the $E_1$ transition, where the strongest change in the spectral shape appears when the surface changes from P terminated to In terminated. Therefore, the maximum at 3.2 eV in the spectrum of the $(2\times1)$ reconstructed surface has been tentatively associated with transitions involving phosphorus dimers at the surface.[9] While the features $A^1_{(2\times4)}$ and $A^3_{(2\times4)}$ could be correlated to surface transitions by theoretical calculations,[11] the authors were not able to reproduce the fine structure, e.g., $A^2_{(2\times4)}$. At the moment, calculated RA spectra for the P-covered $(2\times1)$-like reconstructed surface are not available.

### B. Temperature-dependent energy shifts

The bulk dielectric function was not available for all temperatures investigated here. Therefore, the temperature-dependent shift of the most pronounced features of the SDA

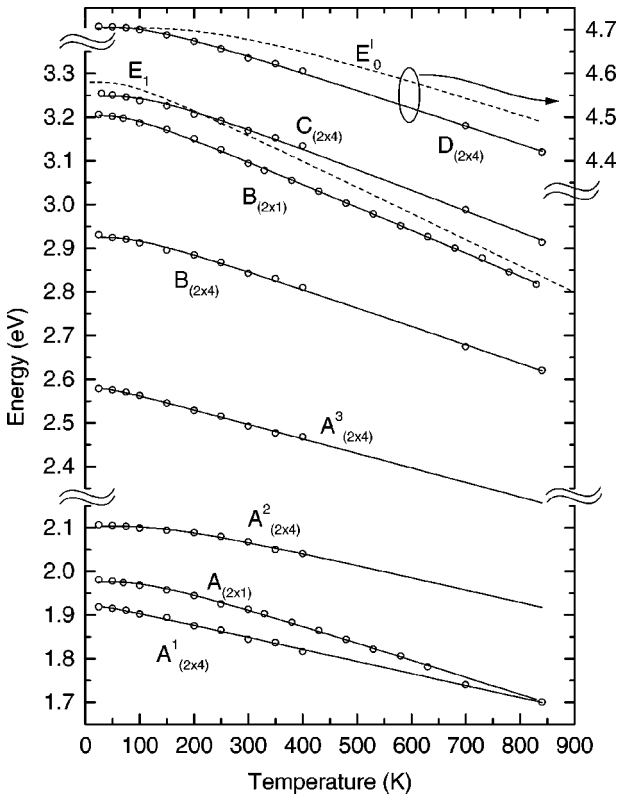


FIG. 4. Temperature-dependent energy shift of the characteristic bulk ($E_1$ and $E_0'$, dashed lines) (Ref. 15) and RAS [$A_{(2\times1)}$ and $B_{(2\times1)}$, $A^1_{(2\times4)} - D_{(2\times4)}$] structures. The solid lines are fits after Eq. (3).

had to be derived directly from the RA spectra. However, it could be verified by comparing SDA and RAS at selected temperatures (e.g., 30 K, 245 K, and 740 K) that there is no significant difference in the temperature behavior of these two signals. To determine the energetic position of the RAS peaks, the more pronounced features labeled *A*, *B*, *C*, and *D* in Fig. 2 were fitted with a Gaussian curve and the center of this fit was used as the energetic position. To determine the temperature dependence of weak peaks (e.g., $A^2_{(2\times4)}$ and $A^3_{(2\times4)}$), the second derivative of the spectrum has been used to determine the position of these structures via a Gaussian fit. This procedure leads to a slightly different absolute energetic position but the temperature dependence remains the same, which was verified for the very low-temperature region. However, reliable data could only be achieved up to 400 K since these spectral features were to weak at higher temperatures.

Figure 4 shows the temperature shifts compared to those of the bulk critical-points $E_1$ and $E_0'$.[15] The data could be fitted with a model proposed by Lautenschlager *et al.*[22] containing the Bose-Einstein occupation factor for phonons:

$$E(T)=E_0-\alpha\left(1+\frac{2}{e^{(\theta/T)}-1}\right). \tag{3}$$

Two effects contribute to the energy shift of the bulk band transitions of semiconductors. The first is due to the thermal expansion of the lattice coupled with the change of electron energies with volume. The second contribution is the direct renormalization of band energies by electron-phonon interactions.[23] The total energy shift can be expressed by the derivatives[22]

$$\left(\frac{\partial E_g}{\partial T}\right)_p=\left(\frac{\partial E_g}{\partial T}\right)_{\text{therm exp}}+\left(\frac{\partial E_g}{\partial T}\right)_V, \tag{4}$$

or, for small T,[14] as

$$\Delta E_g(T)=\left(\frac{\partial E_g}{\partial V}\right)_T\left(\frac{dV}{dT}\right)_P\Delta T+\left(\frac{\partial E_g}{\partial T}\right)_V\Delta T, \tag{5}$$

where the first term describes the change in $E_g$ caused by thermal expansion and the second term is the result of electron-phonon interaction. The contribution of these effects to $E_g(0)$ can be estimated by extrapolating $E_g(T)$ to $T=0$ using its linear dependence at high temperatures. The resulting energy difference for $T=0$ is known as the *renormalization energy* $\Delta E_{rn}$ of the respective band transition. Physically, $\Delta E_{rn}$ describes the coupling strength for the electron-phonon interaction.[14] The respective values for $\Delta E_{rn}$ and the fitting parameters in Eq. (3) can be found in Table I together with the values for the bulk critical points determined by Lautenschlager *et al.*[15]

TABLE I. Fitting parameters to Eq. (3) for the temperature-dependent energy shift and renormalization energy of the respective features of the RA spectra compared to those of the bulk critical points $E_1$ and $E_0'$ (Ref. 15) (see Fig. 2). Values in brackets determine the 95% confidence level.

| Point | $E_0$ (eV) | $\alpha$ (meV) | $\theta$ (K) | $\Delta E_{rn}$ (meV) |
|---|---|---|---|---|
| $A^1_{(2\times4)}$ | $1.932\pm0.002$ | $12\pm5$ | $85\pm42$ | 12 |
| $A^2_{(2\times4)}$ | $2.169\pm0.016$ | $65\pm17$ | $449\pm70$ | 50 |
| $A^3_{(2\times4)}$ | $2.599\pm0.005$ | $17\pm8$ | $104\pm43$ | 16 |
| $A_{(2\times1)}$ | $2.033\pm0.006$ | $55\pm7$ | $287\pm29$ | 47 |
| $B_{(2\times4)}$ | $2.982\pm0.006$ | $57\pm8$ | $249\pm33$ | 50 |
| $B_{(2\times1)}$ | $3.264\pm0.003$ | $61\pm4$ | $231\pm15$ | 54 |
| $E_1$ | 3.348(7) | 68(10) | 224(30) | 60 |
| $C_{(2\times4)}$ | $3.312\pm0,009$ | $58\pm11$ | $251\pm44$ | 53 |
| $E_0'$ | 4.867(42) | 163(44) | 775(127) | 106 |
| $D_{(2\times4)}$ | $4.768\pm0,005$ | $60\pm6$ | $291\pm26$ | 52 |

Comparing the temperature-dependent energy shift of the bulk critical points with the respective RAS features nearby, there seems to be only a slight similarity. However, looking at the parameters $\theta$ and $\alpha$ in Table I, one can see a clear similarity within the error of the values for the $E_1$ critical point and the nearby RAS features $B_{(2\times1)}$, $C_{(2\times4)}$, and even $A_{(2\times1)}$. The fitting parameter $\theta$ may be interpreted as a mean phonon frequency[22,14] and is similar in magnitude even for different surface reconstructions. The values for $\theta$ are all in the range of the bulk longitudinal acoustic (LA) phonons.[24] The fitting parameter $\alpha$ is closely related to the renormalization energy $\Delta E_{rn}$. The values for $\Delta E_{rn}$ for the InP bulk transitions $E_0$,[25] $E_0+\Delta_0$,[15,25] and $E_1$[15] are near 50 meV, as are the values for the RAS features mentioned

above. In summary, the RAS features, $B_{(2\times1)}$ and $C_{(2\times4)}$, are similar to the InP bulk transitions in both energetic position and T shift ($\theta$ and $\Delta E_{\mathrm{rn}}$). This strongly suggests that these features are ''intrinsic,'' e.g., caused by transitions involving bulk states (sb, bs, or sm-bb).

The $D_{(2\times4)}$ feature and the $E_0'$ critical point occur at the same energy at low temperatures, but their values for $\theta$ and $\alpha$ are very different. Although our fit shows a good match to the data, there is significant scattering of the data around the fit determined by Lautenschlager *et al.*[15] Furthermore, there is no bulk related phonon with an energy $E=k_B\theta$ corresponding to 775 K (see Table I). The highest values for bulk phonons in InP are near 500 K as determined by Borcherds *et al.*[24] Additionally, the value for $\Delta E_{\mathrm{rn}}$ determined for $D_{(2\times4)}$ is again $\cong 50$ meV in contrast to the value of 106 meV derived from Lautenschlager's fit. Further work seems necessary to clarify this point.

In contrast to the other features, there is no bulk transition in the vicinity of the low energy peaks near 1.9 eV, namely the $A^1_{(2\times4)}-A^3_{(2\times4)}$, and $A_{(2\times1)}$ features. However, as seen in Fig. 4 and Table I, these features show a different behavior. The temperature dependence of the $A_{(2\times1)}$ peak shows a similar behavior compared to the features in the vicinity of the bulk transitions. In addition, other experiments[26,27] have shown that this peak is sensitive to changes in the surface chemistry as well. A possible explanation for this phenomenon could be a bs or sb-like transition to produce the $A_{(2\times1)}$ structure, e.g., a transition involving both bulk and surface related states. On the other hand, the $A^1_{(2\times4)}-A^3_{(2\times4)}$ peaks behave significantly different. For the $A^1_{(2\times4)}$ and $A^3_{(2\times4)}$ peaks, the flattening of the fit curve in the low-temperature region is significantly reduced so that the curve may be regarded as linear. The corresponding values for $\theta$, $\alpha$, and $\Delta E_{\mathrm{rn}}$ are much lower than the others in Table I. Their values for $\theta$ correspond to the transversal acoustic phonons.[24] The $A^2_{(2\times4)}$ feature shows an unexpected temperature behavior, varying drastically from its neighboring peaks. The flattening of the curve occurs at much higher temperatures. Here, the value for $\theta=449$ K corresponds to the transversal optical phonons. To understand the behavior of these peaks one has to take a closer look at the photon-phonon coupling at the surface. Unfortunately, a detailed surface phonon band structure is not yet available for the InP(100) surface. The value for $\Delta E_{\mathrm{rn}}$ of $A^2_{(2\times4)}$ lies in the range of the bulk transitions. Therefore, it would be interesting to know if theoretical calculations with a higher resolution could resolve this peak in the calculated RA spectrum of the $(2\times4)$ reconstructed surface, or if it has a different and more complex origin.

## IV. SUMMARY

We have performed RAS measurements on different reconstructed InP(100) surfaces between 20 and 840 K. At low temperatures, the spectral features showed significant blue shifts and sharpening compared to features in spectra taken at higher temperatures due to the reduced lattice constant and electron-phonon interactions. Some new features appeared in the spectrum obtained from the $(2\times4)$ reconstructed surface. From a line-shape analysis, the intermediate phase could be determined as consisting of domains of $(2\times4)$- and $(2\times1)$-like reconstructed surfaces.

The temperature shift of the energetic positions for representative features in the RA spectra was fitted using a model containing the Bose-Einstein occupation factor for phonons. Comparing the fitting parameters and the renormalization energy of the respective RAS features with those of bulk critical point transitions nearby, we found that all RAS features above 2.8 eV in the vicinity of bulk transitions are most likely ''intrinsic,'' e.g., surface modified bulk related structures. The minimum of the P-rich surface shows a behavior similar to the peaks in the high-energy region and therefore seems to be related to a transition involving both bulk and surface states. On the other hand, the minimum of the well-ordered In-rich $(2\times4)$ reconstructed surface shows a different temperature dependence. Furthermore, two peaks show a negligible coupling to the bulk phonons as indicated by their low values of the renormalization energy $\Delta E_{\mathrm{rn}}$, which makes them most likely to originate from pure surface transitions.

## ACKNOWLEDGMENT

S.V. thanks his colleagues at the Department of Chemical Engineering at UCLA for worthwhile discussions and critical review of the manuscript.

*Corresponding author. Present address: Chemical Engineering Department, University of California, Los Angeles CA 90095; electronic address: visbeck@ucla.edu

†Present address: Ferdinand-Braun-Institut für Höchstfrequenztechnik, Albert-Einstein-Str. 11, D-12489 Berlin, Germany.

[1] L. J. Mawst, A. Bhattacharya, J. Lopez, D. Botez, D. Z. Garbuzov, L. DeMarco, J. C. Connolly, M. Jansen, F. Fang, and R. F. Nabiev, Appl. Phys. Lett. **69**(11), 1532 (1996).

[2] A. W. Bett, F. Dimroth, G. Stollwerk, and O. V. Sulima, Appl. Phys. A: Mater. Sci. Process. **69**, 119 (1999).

[3] T. Takamoto, E. Ikeda, and H. Kurita, Appl. Phys. Lett. **70**, 381 (1997).

[4] F. Hyuga, T. Aoki, S. Sugitani, K. Asai, and Y. Imamura, Appl. Phys. Lett. **60**(16), 1963 (1992).

[5] T. Kobayashi, K. Taira, F. Nakamura, and H. Kawai, J. Appl. Phys. **65**(12), 4898 (1989).

[6] M. D. Williams, A. L. Greene, T. Daniels-Race, and R. M. Lum, Appl. Surf. Sci. **157**, 123 (2000).

[7] T. Nittono and F. Hyuga, J. Appl. Phys. **81**(6), 2607 (1997).

[8] T. Hannappel, S. Visbeck, K. Knorr, J. Mahrt, M. Zorn, and F. Willig, Appl. Phys. A: Mater. Sci. Process. **69**(4), 427 (1999).

[9] M. Zorn, T. Trepk, J.-T. Zettler, B. Junno, C. Meyne, K. Knorr, T. Wethkamp, M. Klein, M. Miller, W. Richter, and L. Samuelson, Appl. Phys. A: Mater. Sci. Process. **65**, 333 (1997).

[10] K. B. Ozanyan, P. J. Parbrook, M. Hopkinson, C. R. Whitehouse, Z. Sobiesierski, and D. I. Westwood, J. Appl. Phys. **82**(1), 474 (1997).

[11] W. G. Schmidt, N. Esser, A. M. Frisch, P. Vogt, J. Bernholc, F.

Bechstedt, M. Zorn, Th. Hannappel, S. Visbeck, F. Willig, and W. Richter, Phys. Rev. B **61**(24), R16 335 (2000).
[12] V. L. Berkovits, P. Chiaradia, D. Paget, A. B. Gordeeva, and C. Goletti, Surf. Sci. **441**, 26 (1999).
[13] D. E. Aspnes and A. A. Studna, Phys. Rev. Lett. **54**(17), 1956 (1985).
[14] P. Y. Yu and M. Cardona, *Fundamentals of Semiconductors: Physics and Materials Properties* (Springer-Verlag, Berlin, 1996).
[15] P. Lautenschlager, M. Garriga, and M. Cardona, Phys. Rev. B **36**(9), 4813 (1987).
[16] T. Hannappel and F. Willig, German Patent No. DE 19 837 851 (1999).
[17] K. Haberland, P. Kurpas, M. Pristovsek, J.-T. Zettler, M. Weyers, and W. Richter, Appl. Phys. A: Mater. Sci. Process. **68**(3), 309 (1999).
[18] D. E. Aspnes, J. Opt. Soc. Am. **63**, 1380 (1973).
[19] P. Vogt, Th. Hannappel, S. Visbeck, K. Knorr, N. Esser, and W. Richter, Phys. Rev. B **60**(8), R5117 (1999).
[20] M. J. Begarney, C. H. Li, D. C. Law, S. B. Visbeck, Y. Sun, and R. F. Hicks, Appl. Phys. Lett. **78**(1), 55 (2001).
[21] L. Li, Q. Fu, C. H. Li, B.-K. Han, and R. F. Hicks, Phys. Rev. B **61**(15), 10 223 (2000).
[22] P. Lautenschlager, P. B. Allen, and M. Cardona, Phys. Rev. B **31**(4), 2163 (1985).
[23] M. L. Cohen and D. J. Chadi, *Semiconductor Handbook* (North-Holland, Amsterdam 1980), Vol. 2, Chap. 4b.
[24] P. H. Borcherds, G. F. Alfrey, D. H. Saunderson, and A. D. B. Woods, J. Phys. C **8**, 2022 (1975).
[25] Z. Hang, H. Shen, and F. H. Pollak, Solid State Commun. **73**(1), 15 (1990).
[26] T. Hannappel, L. Töben, S. Visbeck, H.-J. Crawack, C. Pettenkofer, and F. Willig, Surf. Sci. **470**, L1 (2000).
[27] D. Law, Q. Fu, S. Visbeck, Y. Sun, and R. F. Hicks (unpublished).